Doppler VOR PERFORMANCE WHEN LOCATED 125-FEET ABOVE THE GROUND

Simbo A. Odunaiya, Ph.D.
Ohio University
Athens, Ohio 45701
Fax: +1 740 593-1604
Email: odunaiya@bobcat.ent.ohiou.edu

Fred Gomez, ANI-90
Federal Aviation Administration
800 Independence Ave,
Washington, DC
Fax: +1 202 493-5037
Email: Fred.Gomez@faa.gov

ABSTRACT

The relocation of a Doppler VOR at the Minneapolis-St. Paul International Airport (MSP) and the attendant performance problems that ensued had led to a modeling study and analysis of the system. The VOR performance has been analyzed using an electromagnetic model based on Geometrical Theory of Diffraction (GTD), which takes into consideration the counterpoise size and height above the ground. Due to variations in ground plane as seen by different antennas and the environment, variations in the signal level at the aircraft occur. These variations can result in variations in the 9960 AM signal modulations and in the bearing information. The amount of AM predicted is a function of counterpoise size, the height of the counterpoise above ground, and the environment.

This paper shows that the signal minimums measured during flight checks are consistent with those predicted by the analysis model. The results obtained also indicated that the performance of the VOR was affected more by the height of the counterpoise above ground than by the counterpoise size or the environment. These results are applicable and will be useful for future VOR sitings.

BACKGROUND

The Minneapolis-St. Paul International Airport (MSP) is undergoing an extensive 2010 Expansion Program, which includes the building of a new Runway 17/35. In order to construct the new runway the terminal VOR was required to be relocated. The FAA believed that an elevated DVOR would be required at the airport to provide the best coverage given the existing siting conditions. To find available real estate to support the VOR, it was relocated to the top of a new terminal parking garage and converted to a Doppler system. Before the installation of this Doppler VOR, the FAA Technical Center performed a mathematical modeling analysis, which determined that Air Traffic Control requirements for this VOR (mainly the 51- and 71-degree radials) supporting arrivals and departures at MSP could be met utilizing the parking garage. Based upon this analysis a 75-foot diameter counterpoise was installed at a height of 125 feet above ground level (AGL). The new DVOR was completed in spring 2001. Subsequently, flight inspection determined that the signal-in-space did not meet requirements for bearing error and frequency modulation deviation. The FAA requested Ohio University perform an analysis to determine the cause of the deficient

radiated signal. There are seven Doppler VORs operating on 52-foot counterpoises without radiated signal problem; however, these VORs are nominally only 15-feet above the ground. This paper details the results obtained from the study. Results of the several flight checks performed on the system are also included.

MODEL FORMULATION

Near Zone Basic Scattering Code

Since the MSP Doppler VOR is located at 125 feet AGL, the existing VOR model, the Ohio University VOR Performance Prediction Model[1] was found to be inadequate for the analysis. This code assumes that an ideal signal is radiated by the Doppler antenna and as such does not provide accurate results for this analysis. An all-purpose Electromagnetic code, the Near Zone Basic Scattering Code (NZBSC)[2] that was developed by the ElectroScience laboratory at The Ohio State University was used to develop this model. The original version of this code was developed in the 1970s to analyze radiation patterns of antennas that were mounted on aircraft surfaces and structures. The version used in the development of this model, is the windows version, NZBSC 3.4, which was developed for use by the National Aeronautics and Space Administration (NASA) for analysis of antennas mounted on space stations. The code made use of the Geometrical Optics (GO) and the Uniform Theory of Diffraction (UTD) electromagnetic theories. The NZBSC is capable of modeling single edge, double edge, curved edge, corner, and slope diffraction mechanisms. This ability is very helpful in modeling the polygonal counterpoise (Figure 1) that was used at MSP.

The NECBSC input includes the geometry of the source, the scatterers, and the flight path. Each of the Doppler antennas was modeled as a circular loop antenna.

Figure 1 Photo of relocated VOR showing geometry of counterpoise

Figure 2 is a diagram depicting the modeled Doppler antennas. The NECBSC input file was generated specifically for a Doppler VOR to include all 50 sideband antennas as well as the center carrier antenna, along with a ground-plane size and shape similar to the installed counterpoise (Figure 2). The Output of the NZBSC code gives the radiation patterns or the near zone electric field strength of the counterpoise mounted VOR antennas. The output of this composite signal was then processed through the existing receiver algorithm that only provides bearing error output. The receiver processing algorithm was then modified to provide the amplitude modulated output of the 9960-Hz signal.

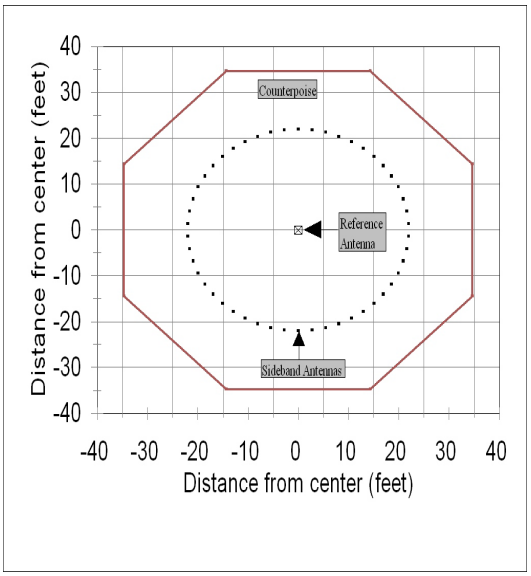

Figure 2. Diagram depicting geometry of Doppler antennas and counterpoise.

Doppler Processor

The post processor used in this model performs two major functions. One is to compute the modulation percentage of the received 9960 Hz signal while the other function computes the VOR azimuth error.

9960 Hz Modulation

Figure 3 shows a typical Aircraft VOR receiver. The total signal received by this receiver corresponds to the vector sum of the direct and reflected signals. The reflected signals affect the 9960 Hz modulation signals received at the receiver. In the case of the Doppler VOR, there are space dependent differences in the multipath environment for the carrier and sideband signals, whose ratio determines the modulation percentage. These differences cause actual variation in the modulation percentage. In order to model the percentage modulation for the 9960 Hz signal the output of the 9960 Hz filter in Figure 2 is analyzed.

The carrier envelope at the output of the IF stage can be described as

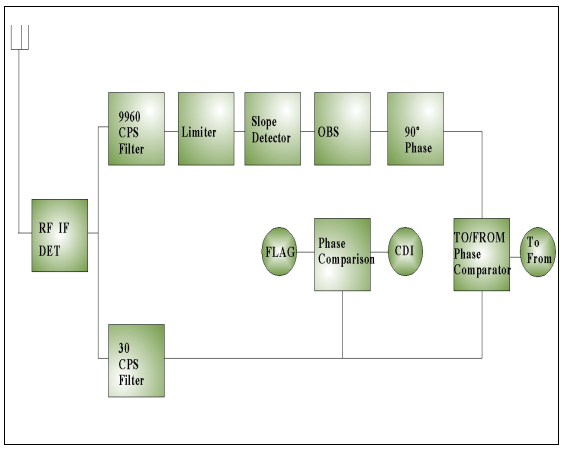

Figure 3. Typical Aircraft receiver.

$$A_1(t) = \left[(C + S(t))(C^* + S^*(t)\right]^{1/2} = a_0(t) + a_1(t) \qquad (1)$$

In the equation above, C and S are the carrier and sideband envelopes and can be written as

$$C = \sum_p C_p e^{j\phi_p}$$
$$S(t) = \sum_p S_p(t) e^{j\phi_p} \qquad (2)$$

The sideband envelope can be represented as a one term Fourier series as follows:

$$S_p(t) = S_p U(t) \qquad (3)$$

where $U(t) = \cos(2\pi ft)$

Considering multipath from various objects, the sideband can be written as

$$a_1(t) = \sum_p S_p U(t) \cos(\phi_p - \theta_1) \qquad (4)$$

where

$$\theta_1 = \tan^{-1}\left(\frac{\sum_p C_p \sin\phi_p}{\sum_p C_p \cos\phi_p}\right) \qquad (5)$$

Doppler effects are included when the output of the filter is properly analyzed. The audio frequency output from the 9960 Hz signal filter can be expressed as

$$V_f(t) = \int_0^\infty h_f(\tau) V_{AF}(t - \tau) d\tau \qquad (6)$$

If the frequency response of the filter is

$$H_0(f) = sinc(\pi fT) \qquad (7)$$

then, the 9960 Hz signal can be expressed as

$$V_{9960}(t) = H_{9960}[V_{AF(t)}] \qquad (8)$$

Signal components at the input of the filter will contain typical terms such as

$$a_p U(t) \cos(\phi_p - \theta_1) = 1/2\, a_p \times (\cos(2\pi ft + \phi_p(t) - \theta_1(t)) + \cos(2\pi ft - \phi_p(t) + \theta_1(t))) \qquad (9)$$

The output from the filter will have two basic components, a contribution from the average carrier level received by signal

paths with large Doppler shifts, and the contributions from the modulation at the filter frequency. These are

$$V_A(t) = \sum_p a_{0p} H_0(f + (\phi_{p'} - \dot{\theta}_0)/2\pi) \times \cos(\pi f T + \theta_0 - \phi_p) \quad (10)$$

where

$$\phi_{n'p} = \frac{d\phi_{np}}{dt}$$

$$\dot{\theta}_n = \frac{2\pi}{\lambda}\frac{dR}{dt}$$

and

$$V_B(t) = \sum_p a_{1p} H_0\left(\frac{(\phi_p - \theta_1)}{2\pi}\right)\cos 2\pi f t \quad (11)$$

The total detected signal at the modulation frequency 9960 Hz, is the sum of the contributions of Equation (10) and Equation (11) above. Assuming that the relative phases of Equation (10) and Equation (11) above are random, then the final rectified output can be regarded as the r.m.s. envelope of the addition of the two expressions. The final expression for the filter output is thus written as:

$$V_f = \left[\Sigma a_{0p}^2 H_0\left(f + \frac{\phi_{p'} - \dot{\theta}_0}{2\pi}\right)^2 + \left(\sum_p a_{1p}\cos(\phi_p - \theta_1) H_0\left(\frac{\phi_{p'} - \dot{\theta}_1}{2\pi}\right)\right)^2 \right]^{1/2} \quad (12)$$

Once the 9960 Hz signal is computed, the modulation percentage can be obtained from the ration of the signal obtained and the carrier signal.

Bearing Error

The Doppler VOR bearing error is computed using the method suggested by Anderson and Flint [3], which has also fully been developed by Odunaiya [4]. Anderson and Flint expressed the error caused by a single reflector situated at a bearing 90 degrees from the Doppler VOR as

$$\psi \approx \frac{2A J_1\left[2\beta_2 r \sin\left(\frac{90^o - \phi}{2}\right)\right]}{\beta_2 r} \times \cos\left(\frac{\phi - 90^o}{2}\right)\cos(\beta_2(r_o - r_1) - \delta) \quad (13)$$

In the equation above **A** is the ratio of the reflected signal to the direct signal from the given scatterer, **r** is the radius of the circle of Doppler antennas, $\mathbf{r_0}$ is the direct path distance from the antenna to the observation point, r_1 is the indirect path distance to the observation point via the reflecting object, δ is the RF phase change caused by the reflector, β_2 is the phase constant at the VOR operating frequency, and J_1 denotes the Bessel function of the first kind of order 1.

It has been shown by Odunaiya that the general formula for the azimuth error on a Doppler VOR for many reflectors located at any azimuth can be expressed as

$$\psi \approx \tan^{-1}\left[\sum_{i=1}^{N} 2A_i\cos[\theta_0 - \theta_1]x \; J_1\left(2\beta_2 r \sin\left(\frac{\phi_i - \phi_0}{2}\right)\right)\cos\left(\frac{\phi_0 - \phi_i}{2}\right) x\, 1/Q\right] \quad (14)$$

where

$$Q = \beta_2 r + \sum_{i=1}^{N} 2A_i\cos[\theta_0 - \theta_1]x \; J_1\left(2\beta_2 r \sin\left(\frac{\phi_i - \phi_0}{2}\right)\right)\sin\left(\frac{\phi_0 - \phi_1}{2}\right) \quad (15)$$

MODEL RESULTS

Considering that the VOR antenna is located 125 feet above ground, the concern is that several signal minimums will result. Also, in the original configuration the 50 sideband antennas are located on a 22-foot radius circle, while the counterpoise itself is 37.5-foot radius, which means that there is only 15 feet of ground-plane under the antennas when the aircraft is at the azimuth angle relative to that antenna. The model was used to predict the vertical

pattern. Due to the height above ground, vertical lobes are caused at various elevation angles resulting in signal minimums with nulls. Figure 4 shows predicted signal level versus elevation angle given the existing 75-foot diameter counterpoise, and also with 150-, and 300-foot diameters. As seen from this figure, the nulls or minimums become less apparent as the counterpoise size increases. Based on these calculations, there is sufficient signal level with the existing counterpoise, but there are a lot of nulls that could potentially intensify bearing errors.

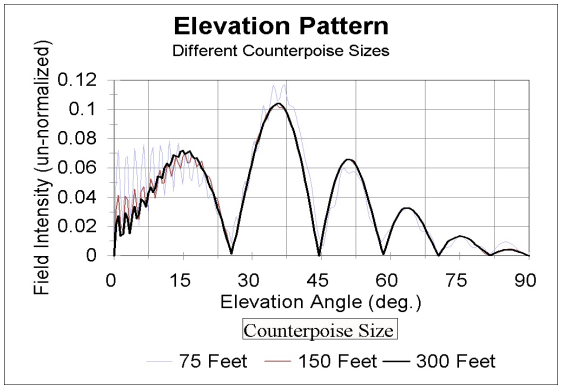

Figure 4. Vertical pattern of signal in space

Since the ground plane varies significantly for each antenna relative to the aircraft, variations in signal level occur which cause oscillations in the signal level received at the aircraft. These variations can result in frequency modulation deviations within the receiver ultimately resulting in bearing errors. The 9960-Hz amplitude modulation (AM) will also be affected by this variation. The amount of AM predicted is a function of counterpoise size and height above ground. Figure 5 shows these variations with respect to counterpoise size.

Bearing Error and Modulation Percentage

This study also considered reflections caused by buildings in the vicinity of the VOR. The buildings are potential causes of errors and modulation variations within

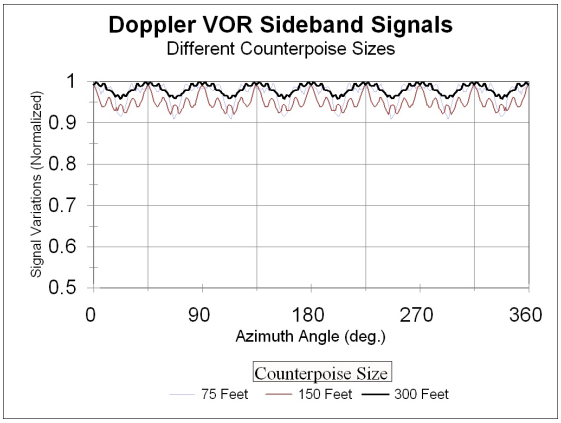

Figure 5. Modulation effect of counterpoise size

the receiver. The structures considered in this modeling effort are as shown in Figure 6. Figure 7 shows the direct and scattered field produced by these buildings for different counterpoise sizes. When all the buildings were included in modeling the VOR scenario, the following results were obtained.

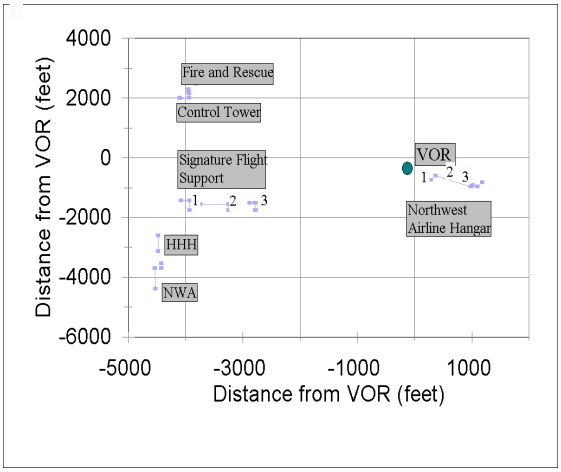

Figure 6. Modeled Buildings

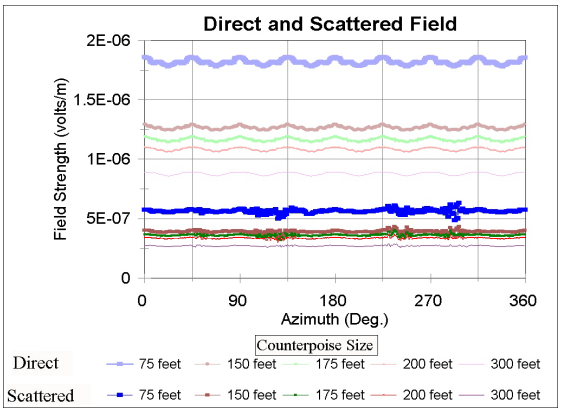

Figure 7. Comparison of direct and scattered fields for various counterpoise sizes

Figure 8 compares the orbital error obtained for the different counterpoise sizes. This result shows that the error obtained with a 300-foot diameter counterpoise is much less than what was obtained for both the 75- and 150-foot diameter counterpoises. However, the differences noted in the error between other sizes of counterpoise are not significant. Figure 9 is the radial error obtained along the 290-degree radial.

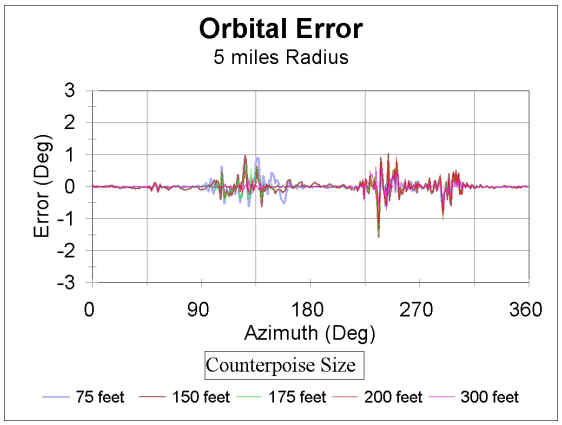

Figure 8. Predicted orbital error for 75-, 150-, 200-, and 300-foot diameter counterpoise

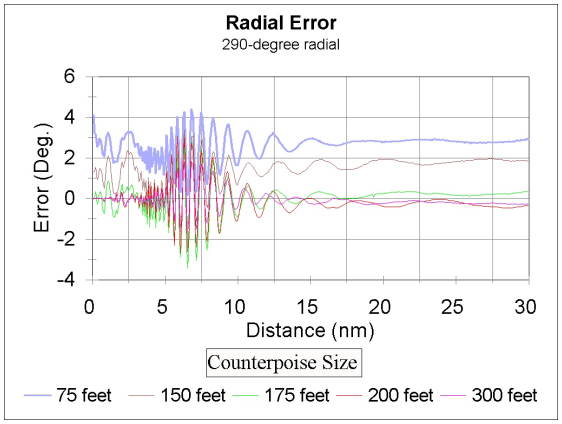

Figure 9. Predicted error for 75-, 150-, 200-, and 300-foot diameter counterpoise along the 290-degee radial

The model has also been used in a similar manner to analyze the effect of the environment on the modulation percentage. Figure 10 shows the 9960-Hz modulation percentage results from the model. Clearly, the modulation percentage is more stable with a counterpoise size of 300 feet. Note again, however, that the results obtained for other counterpoise sizes are not much different from those obtained for the 75-foot case. The results for all counterpoise sizes are also within tolerance limits.

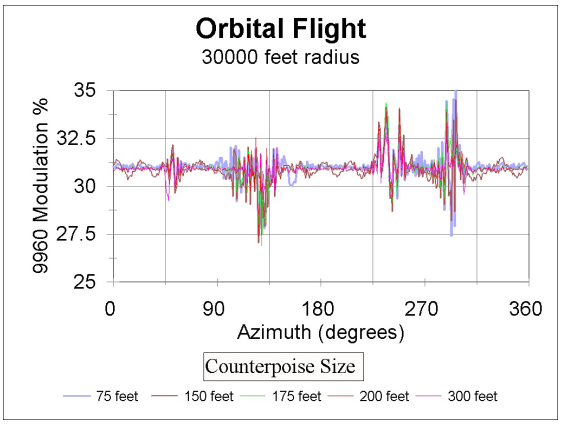

Figure 10. Predicted modulation percentage for 75-, 150-, 200-, and 300-foot diameter counterpoise

Figure 11 gives the results obtained for the modulation percentage on the 290-degree radial. This scenario was run to see what happens on a radial exhibiting significant roughness. In these results, it is clear that the modulation percentage becomes progressively less as the counterpoise size is increased. In this case, the result for the 150-foot diameter counterpoise is clearly better than that for the 75-foot counterpoise. However, the result for the 300-foot counterpoise is the best and highly invariant.

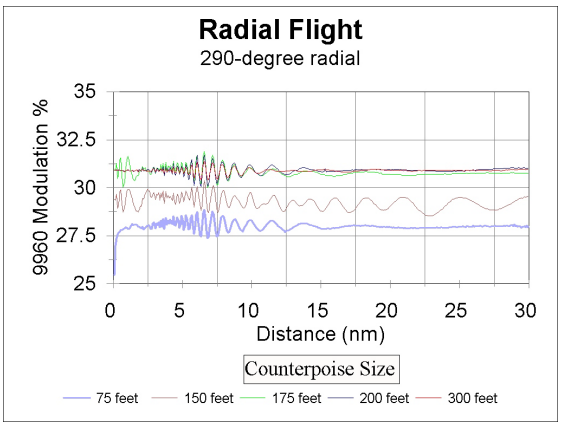

Figure 11. Predicted modulation percentage along the 290-degrees radial for 75-, 150-, 200-, and 300-fott diameter counterpoise

Coverage and Power Density Plots

Considering again the fact that the relocated VOR at MSP is located very high above ground, it is pertinent to investigate what the effect of this height is on the performance of the VOR. ICAO specifications stipulate the minimum sensitivity for the VOR receiver to be -107dBW, while the United States national standard is –120dBW[5]. This requirement is used as a measure of the least acceptable signal available to the receiver. The result obtained for a 75-foot counterpoise located 125 feet above average ground is as shown in Figure 12. This result shows that the signal level goes below -120dBW at around 25 miles from the VOR for a flight level at 5,000 feet AGL. Flights done at 10,000 feet AGL and 18,000 feet AGL do not go below the sensitivity level until around 50 nautical miles from the VOR.

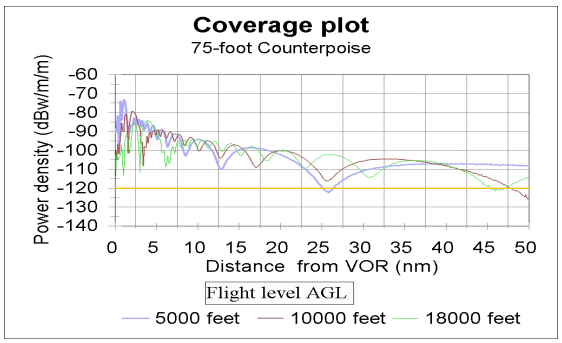

Figure 12. Coverage plot for 75-foot counterpoise at different flight altitudes

A number of different counterpoise sizes are modeled at 125 feet AGL with a flight run at 5000 feet AGL. Figure 13 shows that basically the sensitivity level went below -120 dBW with all the different counterpoise sizes. Again all the counterpoise sizes were modeled for a flight run at 10,000 feet AGL and the results (see Figure 14) indicate that all the runs are above the sensitivity level until close to 50 miles again. There are some discontinuities noted around seven nautical miles which are attributable to edge effects due to the modeling technique used.

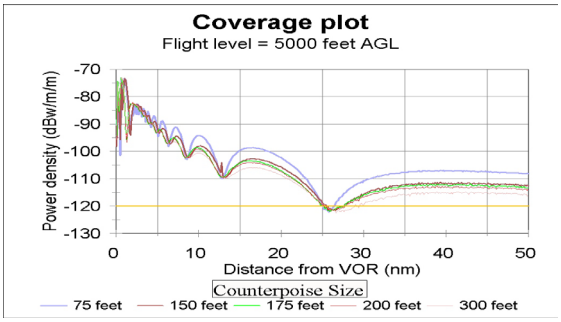

Figure 13. Coverage plot for various counterpoise sizes flown at 5000 feet AGL

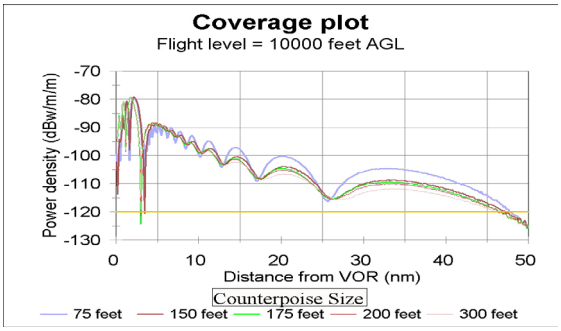

Figure 14. Coverage plots for various counterpoise sizes flown at 10000 feet AGL

In Figure 15, the 75-foot counterpoise is modeled at various heights above the average ground (125, 100, and 75 feet). The results show that the sensitivity level gets better as the height is reduced. The hole created near 25 nmi at a counterpoise height of 125 feet now moves closer to 20 miles and 15 miles for counterpoise heights of 100 feet and 75 feet, respectively. them even beyond 50 miles from the VOR. The results shown in Figure 17 indicate that the 175-foot diameter counterpoise presents a slightly better result than the other two, which is of course expected.

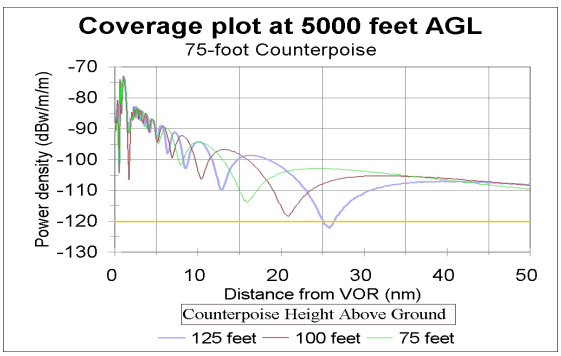

Figure 15. Covergae plot for 75-foot counterpoise located at various heights above ground

FLIGHT CHECK RESULTS

In all of the coverage model results, it is very clear that significant holes are created in the overall pattern. These holes become very significant because of the environment where there are buildings that are capable of degrading VOR performance by reflecting signals. In fact, an examination of the flight check results shows that the out-of-tolerance VOR errors only occur around the positions where minimums are created in the coverage (holes). The lower the height above ground at which the counterpoise is located, the more manageable the holes in the coverage become. The developed model did not predict these out-of-tolerance bearing errors because of the basic assumption in the code that the minimum discernible signal is available. When the required signal is not available, as it is around the nulls in this case, the receiver breaks down and significant bearing error results.

Figures 16, 17, 18, and 19 are extracts from the flight check data. These figures show the bearing error and the AGC for two different runs. Note that where there are nulls or holes, there are also significant VOR errors in each of the runs.

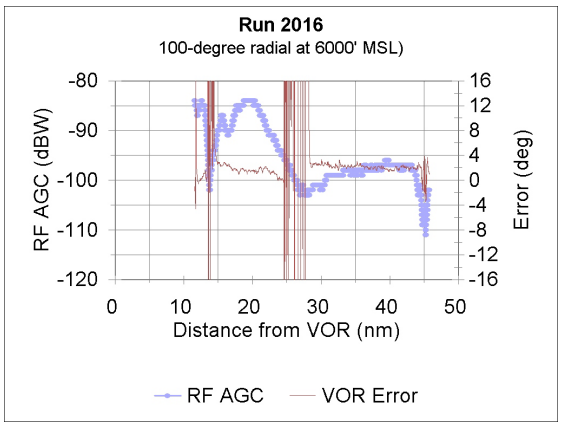

Figure 16. NASE Flight data run 2016 showing Error and AGC curves

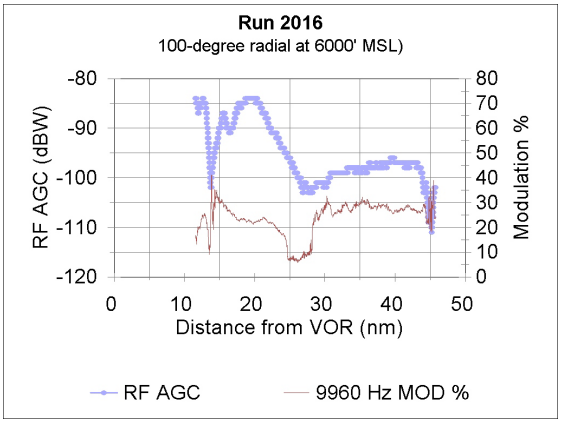

Figure 17. NASE flight data run 2016 showing modulation and AGC curves

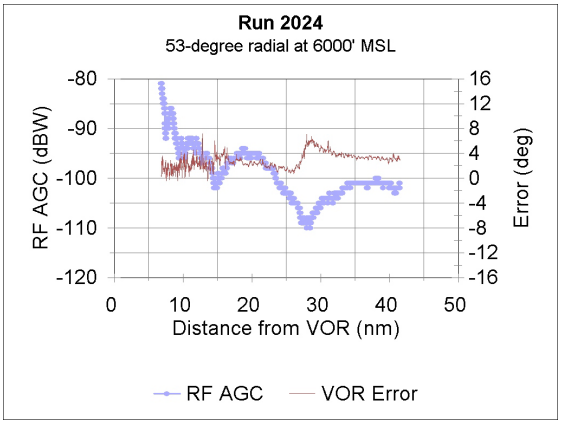

Figure 18. NASE flight data run 2024 showing error and AGC curves

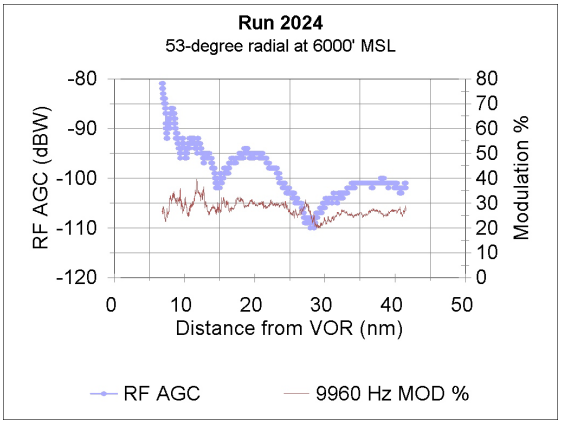

Figure 19. NASE flight data run 2024 showing modulation and AGC curves

CONCLUSION

Based on the modeling analysis and the flight check results, the following conclusions are reached.

1. Variations in the amplitude modulation with the 9960-Hz signal is a function of the counterpoise size and height above ground.

2. The existing buildings around the VOR contribute to both the error and modulation percentage but not at a level that will take the system performance out of tolerance limits, except when there are holes in the signal coverage.

3. The predicted modulation percentage is clearly within tolerance for both orbital flight and radial flight with a 75-foot diameter counterpoise for the model; but it is out-of-tolerance for the flight checks. This results because receiver sensitivity is not considered in the model.

4. The height of the counterpoise above the ground level affects the VOR performance more than does the size of the counterpoise.

RECOMMENDATIONS

From study results, it is apparent that the height above ground level (i.e., 125 feet AGL) exposes the MSP VOR to more roughness in bearing error and modulation percentage. Further, the results show that increasing the counterpoise size from the present 75-foot diameter will not mitigate this problem unless the height above ground level is reduced as well. Therefore, it is recommended that the height above ground level be reduced to a maximum of 100 feet AGL. It is also recommended that future sitings of Doppler system above 100 feet should only be done in a clean environment.

REFERENCES

1.- Odunaiya, Simbo A. and Blazyk Janet M., 'A User's Manual for The Ohio University's VOR Performance Prediction Model Version 3.0," Technical Memorandum OU/AEC 97-32TM00020/3.4-1, Avionics Engineering Center, Ohio University, Athens, Ohio November 1997.

2.- Marhefka R. J., and Burnside W. D., "Numerical Electromagentics Code – Basic Scattering Code (Ver. II) Technical Report 712242-14(713742), Ohio State University Electroscience Laboratory, Ohio State University, Columbs, Ohio, December 1982.

3.- Anderson S. R., and Flint R. B., "The CAA Doppler Omnirange", Proceedings of the IRE vol. 47, No. 5, May 1959, Pp. 808-821.

4.- Odunaiya Simbo, and Sims Gary W., "A Physical Optics Method for Predicting the Effects of Structures on A VOR System", OU/AEC 92-04TM00006/17D-6, Avionics Engineering Center, Ohio University, Athens, Ohio 45701, October 1992.

5.- FAA Order 9840.1 U.S> National Standard for the VOR/DME/TACAN Systems, September 2, 1982.